4450 *Macromolecules* 1993, *26,* 4450-4456

Electronically Conducting Polymers Containing Conjugated Bithiazole Moieties from Bis(thienyl)bithiazoles

Ieuan H. Jenkins and Peter G. Pickup*

Department of Chemistry, Memorial University of Newfoundland, St. John's, Newfoundland A1B 3X7, Canada

Received February 2, 1993; Revised Manuscript Received May 6, 1993

ABSTRACT: Bithiazole-containing polymers prepared by electrochemical polymerization of 5,5′-bis(2-thienyl)-4,4′-dimethyl-2,2′-bithiazole (**Ia**) and 5,5′-bis(3-methoxy-2-thienyl)-4,4′-dimethyl-2,2′-bithiazole (**Ib**) exhibit good conductivities and stable electrochemistry. The redox potential of poly-**Ia** (*ca.* 0.8 V *vs* SCE) is between the values reported for polythiophene and poly(α-bithiophene). The methoxy substituents on the thiophenes of **Ib** increase its solubility and lower the redox potential of the resulting polymer. The morphology, redox potential, and conductivity of poly-**Ib** are strongly influenced by the electrolyte used in the polymerization. The maximum conductivity of poly-**Ib** is *ca.* 0.01 S cm^{-1}, comparable to that of poly(α-terthiophene). It therefore appears that the nitrogen atoms in the conduction pathway have little influence on the redox potential and conductivity of thiophene/thiazole copolymers.

Introduction

The importance of organic conjugated polymers as conductive materials is now beyond question.[1,2] Their many real and potential applications continue to attract a great deal of interest[3,4] and have stimulated the development of a huge range of organic conducting polymers.[1,5]

There has been some interest recently in thiazole-based conjugated polymers.[6-8] Bredas and co-workers[6] have used valence effective Hamiltonian (VEH) calculations, a method known to give very good band structures for sulfur- and nitrogen-containing polymers,[9] to investigate the effect of placing nitrogen atoms in the conduction pathway of a poly(α-thiophene) structure. They conclude that doped polythiazoles should be good conductors. A chemical synthesis,[7] performed by the coupling of the Grignard reagent of 2,5-dibromothiazole, produced an intractable, amorphous brown powder which exhibited a conductivity of about 10^{-7} S cm^{-1} when doped with AsF$_5$. The poor conductivity was attributed to disorder and irregular linkages. The electrochemical polymerization of thiazole is reported to produce a dark-red deposit with an electrical conductivity of 10^{-3} S cm^{-1}.[8] However, in another study it was concluded that neither thiazole nor 4,4′-dimethyl-2,2′-bithiazole could be electrochemically polymerized.[7] A polymer prepared electrochemically from 2,5-bis(2-thienyl)thiazole exhibited a conductivity of 6 × 10^{-5} S cm^{-1},[10] suggesting that the introduction of nitrogen atoms into the polythiophene conduction pathway has a severely detrimental effect on conductivity. There is clearly a need for further experimental studies of thiazole-based systems.

Our interest in thiazole-based polymers stems from their potential to bind transition-metal ions. Coordinated metal sites could be used to increase order in the polymer, to modulate its electronic and electrochemical properties, or to act as catalytic sites for electron transfers. Although the chemistry of conducting polymers with pendant metal complexes is now well developed,[11] there have been few reports of the coordination of metal centers directly to the conjugated backbone of an organic conducting polymer.[12-14]

We report here the synthesis and electrochemical characterization of conducting polymers containing bithiazole moieties as part of the conjugated backbone. These polymers are prepared by the electrochemical polymerization of 5,5′-bis(2-thienyl)-4,4′-dimethyl-2,2′-bithiazole (**Ia**) and 5,5′-bis(3-methoxy-2-thienyl)-4,4′-dimethyl-2,2′-bithiazole (**Ib**). The 2,2′-bithiazole moiety is used to provide bidentate N-donor sites for binding metal ions in future work. The terminal thiophenes facilitate electrochemical polymerization, presumably at their free α positions. This approach to the incorporation of nitrogen donor heterocycles into conducting polymers has previously been used by Kaeriyama and co-workers, who have reported the electrochemical polymerization of 2,6- and 2,5-bis(2-thienyl)pyridine[15] and 2,5-bis(2-thienyl)thiazole.[10]

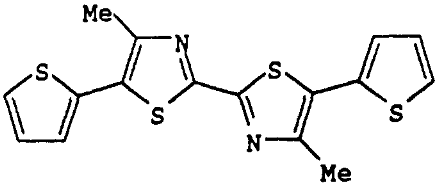

Ia

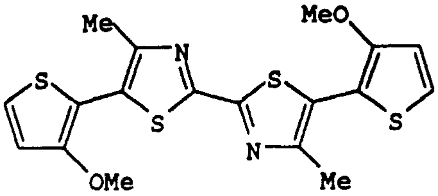

Ib

It was anticipated that **Ia** and **Ib** would give rise to well-defined polymers with well-ordered linkages.[16-18] Coupling at the 4-position of the thiazole is prevented by the methyl substituent (which also simplifies the synthesis of these compounds), and in **Ib** coupling at the 3-position of the thiophene is prevented by the methoxy substituent. The methoxy substituents on **Ib** were also expected to improve its solubility[19] and to reduce the polymer's band gap.[20] Electron density calculations on pyrrole oligomer radical cations[21] suggest that coupling at the 4-positions of the thiophenes of **Ia** and **Ib** will be disfavored. Thus, **Ia** and **Ib** are expected to link predominantly at the thiophene 5-positions, as observed for 1,4-bis(2-thienyl)phenylenes.[18] Then, the symmetric substitution pattern of the monomers will lead to regioregular polymers which

---

* To whom correspondence should be addressed.

should be well ordered and exhibit optimum conductivities.[18]

Experimental Section

Monomer Synthesis. **Ia** and **Ib** were formed by the Negishi[22,23] type coupling of 5,5′-dibromo-4,4′-dimethyl-2,2′-bithiazole with 2-thienylzinc chloride and 3-methoxy-2-thienylzinc chloride, respectively, in the presence of tetrakis(triphenylphosphine)palladium(0). The zinc chloride reagents were prepared by transmetalation, using anhydrous zinc chloride in THF, of 2-thienyllithium and 3-methoxy-2-thienyllithium,[16,24] the latter being formed by lithiation of 3-methoxythiophene at 0 °C.[20] 5,5′-Dibromo-4,4′-dimethyl-2,2′-bithiazole was prepared by the reaction of dithioxamide with chloroacetone,[25] followed by bromination.[26] Melting points were determined using a Fischer-Johns hot-stage apparatus and are uncorrected.

5,5′-Bis(2-thienyl)-4,4′-dimethyl-2,2′-bithiazole (Ia). Anhydrous zinc chloride (11.5 g, 85 mmol) in THF (50 mL) was added to a 1 M solution of 2-thienyllithium in THF (84 mL, 84 mmol) under a nitrogen atmosphere. The mixture was allowed to stir for 1 h before addition of a THF (250 mL) solution of 5,5′-dibromo-4,4′-dimethyl-2,2′-bithiazole (10 g, 28.2 mmol) and tetrakis(triphenylphosphine)palladium(0) (0.65 g, 0.56 mmol, 2 mol %). It was then heated at reflux for 24 h, allowed to cool to room temperature, and quenched with 3 M HCl(aq) (100 mL). Chloroform (500 mL) was added, and the organic layer was separated, washed with water, and dried over magnesium sulfate (5 g). Concentration gave 10 g of a crude solid, which was purified by column chromatography on silica using chloroform as eluent. The desired product (**Ia**) was obtained as an orange powder (2 g, 20%). Mp: 225–228 °C. ^{1}H NMR (300 MHz, $CDCl_3$, ppm *vs* TMS): δ 7.39 (2H, dd, $J_{3,5}$ = 0.9 Hz, $J_{4,5}$ = 4.8 Hz, H-5), 7.22 (2H, dd, $J_{3,5}$ = 0.9 Hz, $J_{3,4}$ = 3.6 Hz, H-3), 7.11 (2H, dd, $J_{3,4}$ = 3.6 Hz, $J_{4,5}$ = 4.8 Hz, H-4), 2.65 (6H, s, $-CH_3$). MS: *m/z* 360 (M^+, 100%), 180 (15), 154 (44), 109 (20). Anal. Calcd for $C_{16}H_{12}N_2S_4$: C, 53.33; H, 3.33; N, 7.77; M^+ 359.9882. Found: C, 52.29; H, 3.24; N, 7.73; M^+ 359.9882.

5,5′-Bis(3-methoxy-2-thienyl)-4,4′-dimethyl-2,2′-bithiazole (Ib). **Ib** was prepared following the procedure for **Ia** utilizing 3-methoxy-2-thienyllithium (26 mmol) (by the lithiation of 3-methoxythiophene with *n*-butyllithium[20]), zinc chloride (3.5 g, 26 mmol), 5,5′-dibromo-4,4′-dimethyl-2,2′-bithiazole (2 g, 5.56 mmol), and tetrakis(triphenylphosphine)palladium(0) (0.35 g, 0.3 mmol). **Ib** was obtained as an orange-red powder (25%) after chromatographic purification (silica/chloroform). Mp: 138–140 °C. ^{1}H NMR (300 MHz, $CDCl_3$, ppm): δ 7.25 (2H, d, $J_{4,5}$ = 5.7 Hz, H-4), 7.91 (2H, d, $J_{4,5}$ = 5.7 Hz, H-5), 3.93 (6H, s, $-OCH_3$), 2.64 (6H, s, $-CH_3$). MS: *m/z* 420 (M^+, 50%), 405 (14), 262 (22), 169 (100), 125 (20). Anal. Calcd for $C_{18}H_{16}N_2O_2S_4$: C, 51.43; H, 3.81; N, 6.66; M^+ 420.0094. Found: C, 51,55; H, 3.82; N, 6.48; M^+ 420.0079.

Reagents. THF was dried by refluxing over calcium hydride. Dithioxamide, chloroacetone, 3-methoxythiophene, *n*-butyllithium, 2-thienyllithium, bromine, tetrakis(triphenylphosphine)palladium(0) were all obtained from Aldrich chemicals and used as received. Zinc chloride was dried at 120 °C under vacuum with stirring for at least 4 h.

Electrochemistry. Electrochemical experiments were performed in conventional three-compartment glass cells at room temperature. Three electrode arrangements consisting of a 0.0079 cm^2 Au disk or a 0.0052 cm^2 Pt disk sealed in glass, a Pt wire counter electrode, and a Ag/AgCl/0.1 M NaCl reference electrode (*ca.* +60 mV *vs* SCE) were used. Electrochemical instrumentation consisted of a Solartron 1286 electrochemical interface, and impedance spectroscopy was performed using a Solartron 1250 frequency response analyzer. For dual-electrode voltammetry,[27] the potentials of two 0.0020 cm^2 Pt disk working electrodes sealed in glass, or two parallel Pt band electrodes[28] (0.10 mm × 1.6 mm, 50 μm apart) sealed in epoxy, were controlled using a Pine Instruments RDE4 potentiostat/galvanostat. Tetraethylammonium perchlorate (Fluka; >99%), tetrabutylammonium hexafluorophosphate (Aldrich; 98%), tetrabutylammonium perchlorate (Fluka; >98%), dichloromethane (Caledon; spectroscopic grade), chloroform (Caledon; spectroscopic grade), and acetonitrile (Fisher; HPLC grade) were used as received.

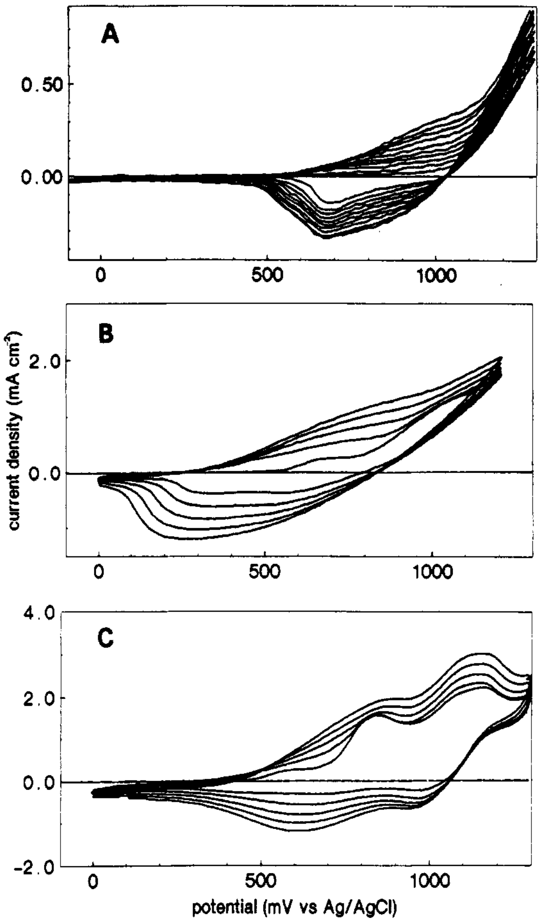

Figure 1. Cyclic voltammograms (100 mV s^{-1}) of (A) 20 mM **Ia** in chloroform containing 0.1 M Bu_4NPF_6 at Au, (B) 20 mM **Ib** in chloroform containing 0.1 M Bu_4NClO_4 at Pt, and (C) 20 mM **Ib** in dichloromethane containing 0.1 M NBu_4NClO_4 at Pt. In all cases currents increase with successive scans.

Scanning Electron Microscopy and X-ray Emission Analysis. Polymer films were examined using a Hitachi S-570 scanning electron microscopy. X-ray emission spectra of films grown on glassy carbon disk electrodes (0.0707 cm^2; Electrosynthesis Co.) sealed in epoxy were collected using a Tracor Northern 5500 energy dispersive X-ray analyzer equipped with a Microprobe 70152 silicon detector.

Results and Discussion

Electrochemical Polymerization. Due to the low solubility of **Ia** in the solvents commonly used for electrochemical polymerizations (acetonitrile, water, nitromethane, nitrobenzene, benzonitrile, dichloromethane), chloroform was found to be the most suitable solvent for preparation of poly-**Ia**. Although more soluble than **Ia** in all solvents tested, **Ib** was still only sparingly soluble in acetonitrile and nitromethane and so was polymerized in chloroform or dichloromethane. Unlike other systems in which a nucleophilic nitrogen is present,[29] **Ia** and **Ib** did not require the addition of acid to electropolymerize.

Figure 1A shows cyclic voltammograms at a gold electrode for a 20 mM solution of **Ia** in chloroform containing 0.1 M Bu_4NPF_6. The monomer begins to oxidize at about +1.0 V. Scanning of the potential up to 1.3 V generates a broad cathodic peak at +0.7 V on the return scan. The increase in the size of this peak, and the corresponding anodic shoulder at 1.0 V, indicates that it is due to an electroactive film formed on the electrode. The polymer film cound be seen on the electrode when it was removed from the cell. The polymer was red in the reduced state and black in the oxidized state, as were films of poly-**Ib**. Poly-**Ia** can also be deposited on Pt.

For **Ib**, the choice of either Pt or Au electrodes and either Bu_4NPF_6 or Bu_4NClO_4 as the supporting electrolyte had little influence on the cyclic voltammetry of the monomer. However, large differences were observed between chloroform and dichloromethane. In chloroform, cyclic voltammograms of **Ib** (Figure 1B) are similar to those of **Ia** (Figure 1A), except that **Ib** is more easily oxidized and the resulting polymer has a lower redox potential because of electron donation by the methoxy substituents. **Ib** begins to oxidize at 0.6 V, exhibiting a small prewave followed by a larger broad wave at 1.0 V. The resulting polymer is reduced in two broad overlapping waves at 0.6 and 0.4 V. In dichloromethane, cyclic voltammograms of **Ib** are quite different (Figure 1C). Two distinct oxidation waves at 0.8 and 1.1 V appear in addition to the prewave at 0.6 V. The wave at 1.1 has a cathodic counterpart at 0.9 V and appears to be close to reversible. The polymer is reduced in a broad wave at ca. 0.6 V. We can offer no explanation of the voltammetry in dichloromethane or why it is so different from that in chloroform.

In the remainder of this work polymer films were grown at constant current so that their thickness could be controlled simply by adjusting the polymerization time. For both polymers a current density of *ca.* 0.25 mA cm^{-2} was found to be optimal. For polymerization of **Ia**, the potential typically dropped from an initial value of *ca.* 1.10 to around 1.06 V after 10 min of polymerization. At substantially higher current densities, the potential increased during polymerization and poor quality films were produced. For **Ib**, the potential typically started at *ca.* 0.80 V at 0.2 mA cm^{-2} and decreased by about 50 mV during 30 min of polymerization.

Cyclic Voltammetry of Poly-Ia and Poly-Ib. Figure 2 shows cyclic voltammograms of poly-**Ia**- and poly-**Ib**-coated electrodes in acetonitrile containing Et_4NClO_4. The poly-**Ia** film (Figure 2A) and the first poly-**Ib** film (Figure 2B) were both grown at constant current in chloroform/Bu_4NPF_6. The second poly-**Ib** film (Figure 2C) was grown in dichloromethane/Bu_4NClO_4. All three films show the broad, fairly featureless regions of high capacitance characteristic of conducting polymers. Peak positions are not very well-defined, nor stable, and therefore provide only rough estimates of redox potentials. Nevertheless, it is clear that poly-**Ib** is more easily oxidized than poly-**Ia** and that poly-**Ib** is more easily oxidized when prepared in dichloromethane/Bu_4NClO_4 rather than chloroform/Bu_4NPF_6. Voltammograms of poly-**Ib** prepared in dichloromethane/Bu_4NPF_6 were similar to those of poly-**Ib** prepared in chloroform/Bu_4NPF_6 (Figure 2B), indicating that the differences between the voltammograms in parts B and C of Figure 2 are due primarily to the different electrolytes used in the polymerization.

Assuming that the capacitive envelopes observed for these materials are due to a series of closely spaced redox waves corresponding to segments of polymer with different conjugation lengths and/or conformations,[2,30,31] the initial redox potentials of the three polymers can be estimated to be 0.7, 0.4, and 0.2 V, respectively. The difference between poly-**Ia** (0.7 V) and poly-**Ib** (0.4 V) can be attributed to the electron-donating effect of the methoxy group. The difference between poly-**Ib** prepared in chloroform/Bu_4NPF_6 (0.4 V) and dichloromethane/Bu_4NClO_4 (0.2 V) may be due to a higher average chain/conjugation length in the latter, to a more regular linkage of the four-ring units, or to morphological differences (see below).

Comparison of the charge under a voltammogram of a polymer film with the polymerization charge provides information about the Coulombic efficiency of the polymerization and/or the degree of oxidation of the polymer. In Figure 2, the charges under the cathodic portions of the voltammograms correspond to 12% (A), 15% (B), and 14% (C) of the respective polymerization charges. Assuming that the voltammetric charge corresponds to 1 electron per four-ring unit (see below) and that the polymerization requires 3.0 electrons per unit (2 electrons for the linkages and 1 to oxidize the resulting polymer), the polymerization efficiency is about 40% in each case. These low efficiencies appear to be an inherent problem in the electropolymerization of oligomers.[32] Presumably, stabilization of the radical cation or the dication by delocalization over the four rings allows diffusion of these intermediates away from the electrode surface to successfully compete with the coupling and precipitation processes.

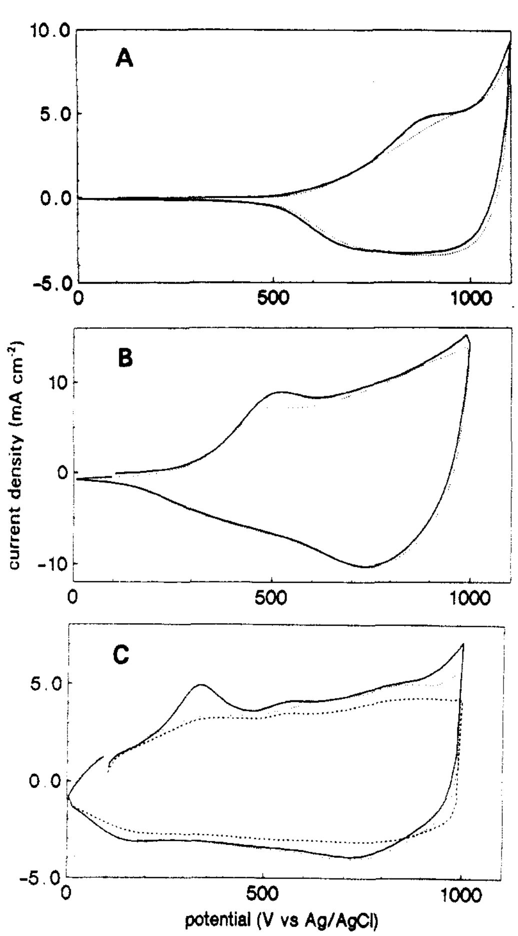

Figure 2. Cyclic voltammograms (100 mV s^{-1}) of poly-**Ia** (A; 0.6 μm thick on Au, prepared in chloroform/Bu_4NPF_6) and poly-**Ib** (B; 3 μm thick on Au, prepared in chloroform/Bu_4NPF_6, and C; 2 μm thick on Pt, prepared in dichloromethane/Bu_4NClO_4) coated electrodes in acetonitrile containing 0.1 (A and B) or 0.2 (C) M Et_4NClO_4. Solid line: 1st scan. Dotted line: 2nd scan. The dashed voltammogram in C was recorded after the impedance measurements shown in Figure 4A. All films were prepared at a constant current (0.13–0.29 mA cm^{-2}).

The thicknesses of poly-**Ia** and poly-**Ib** films can be conveniently estimated from cyclic voltammograms like those shown in Figure 2. The values given in the caption of Figure 2 were calculated by assuming that the charge under the cathodic wave corresponds to 1 electron per four-ring unit and that each polymer has a density of 1.0 g cm^{-3}. These assumptions are semiquantitatively supported by the results in the next section. Although this is a crude estimation of film thickness, it is important in that it allows us to estimate conductivities from resistance measurements on the polymers.

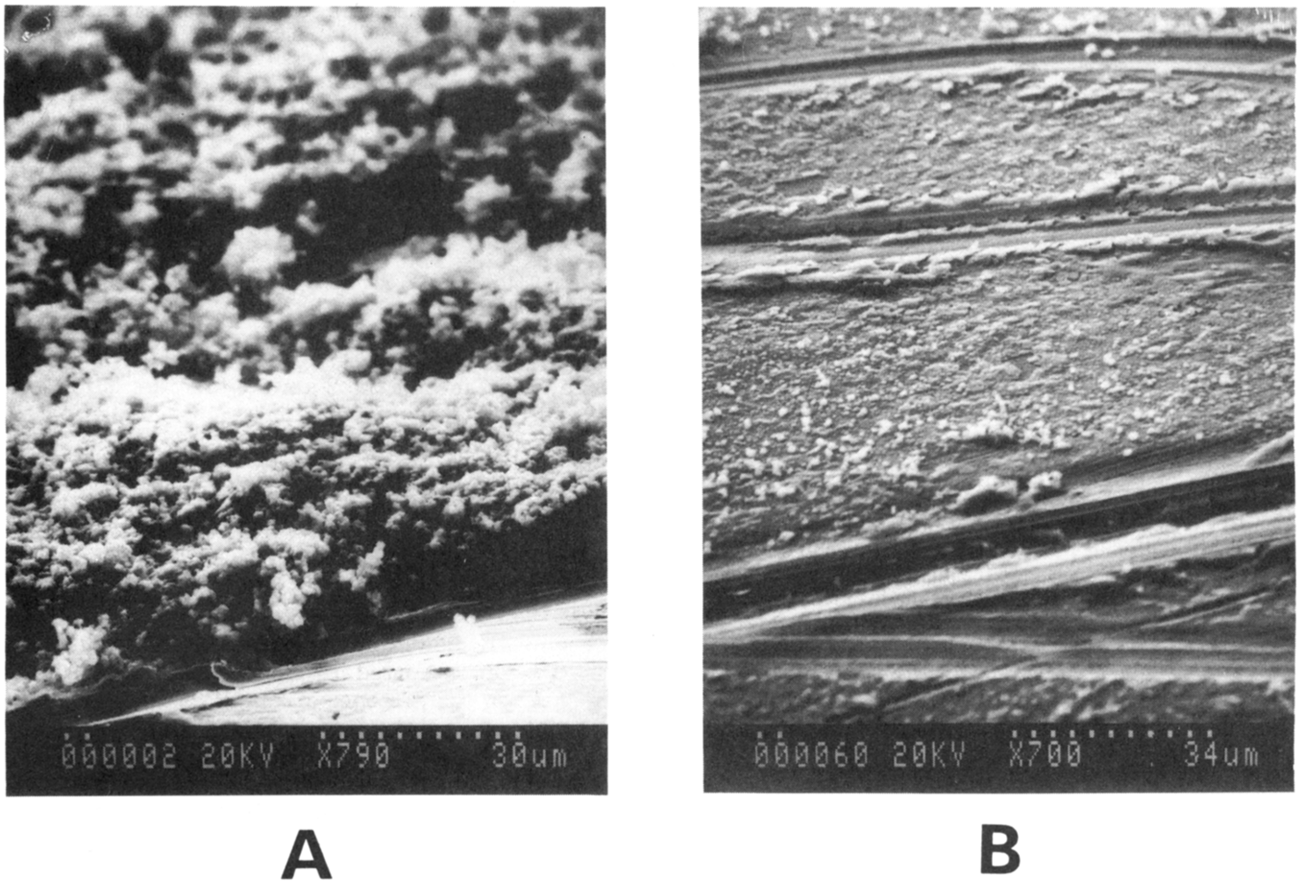

Figure 3. Scanning electron micrographs of poly-**Ia** (A; prepared on Au in chloroform/Bu_4NClO_4 using a charge of 0.42 C cm^{-2}) and poly-**Ib** (B; prepared on Pt in chloroform/Bu_4NClO_4 using a charge of 0.60 C cm^{-2}) coated electrodes. Both coated electrodes have been scraped with a scalpel to reveal the thickness and internal morphology of the film.

Morphology and Degree of Oxidation. Thick films of poly-**Ia** prepared from chloroform/Bu_4NPF_6 appear rough and powdery to the naked eye. Scanning electron microscopy revealed a very granular morphology. Figure 3A shows a poly-**Ia** film deposited on a Au electrode using a charge density of 0.42 C cm^{-2}. The near part of the powdery deposit has been scraped away with a scalpel to reveal an underlying compact polymer layer. Similar two-layer structures have been reported for poly(3-methylthiophene).[33] The formation of the outer powdery layer is probably initiated by the precipitation of oligomers which accumulate in the solution close to the electrode during the polymerization.[33,34] Once this process begins, the precipitate presumably nucleates further electrochemical deposition which leads to the observed porous structure.

A poly-**Ib** film prepared in chloroform containing Bu_4NPF_6 exhibited a two-layer structure similar to that shown for poly-**Ia** in Figure 3A. However, a thick film grown from chloroform containing Bu_4NClO_4 was relatively smooth and compact (Figure 3B). It is not clear why the change in electrolyte produces such a dramatic change in morphology; however, we speculate that changes in the solubilities of the oligomer intermediates are responsible. The scratches in the polymer layer shown in Figure 3B, made using the point of a scalpel, suggest that it is 5–10 μm thick. On the basis of the polymerization efficiency of 40% established above, the film should have a mass of approximately 0.4 mg cm^{-2}. The reported density of polythiophene is ca. 1.5 g cm^{-3},[35] which would correspond to a film thickness of 3 μm. The film is clearly thicker than this and so must be less dense than polythiophene. As a compromise between the observed and expected thicknesses, we have assumed a nominal density of 1.0 g cm^{-3}.

Although films of poly-**Ib** prepared in dichloromethane/Bu_4ClO_4 were not examined by electron microscopy, they appeared smooth and shiny to the naked eye and are therefore presumed to deposit in a compact morphology similar to that shown in Figure 3B. Rough, powdery films like that shown in Figure 3A can clearly be distinguished by their matt appearance.

An estimation of the degree of oxidation of as-formed poly-**Ib** was obtained by X-ray emission (electron microprobe) analysis.[36] Films prepared on glassy carbon electrodes in chloroform containing Bu_4NClO_4 were removed from the polarization cell while still in the oxidized form and thoroughly washed with acetone in order to remove excess electrolyte from the surface. Analysis of two films gave Cl:S ratios of 0.22 and 0.40, respectively, indicating that there is approximately one perchlorate counterion associated with each four-ring unit in the polymer. The average result corresponds to an oxidation level of 0.31 holes per ring, which is within the range reported for polythiophene.[35,36]

Impedance Spectroscopy. Impedance measurements have been used to estimate the *in situ* conductivities of poly-**1a** and poly-**1b** films at various levels of oxidation. Although the primary interest here is in electronic conductivities, impedance measurements also provide information about a polymer's ionic conductivity. The arguments and procedures that we use to extract ionic and electronic resistances from impedance data on conducting polymers are fully discussed elsewhere.[37–39]

Figure 4A shows complex plane impedance plots at various potentials for a poly-**1b**-coated Pt electrode in

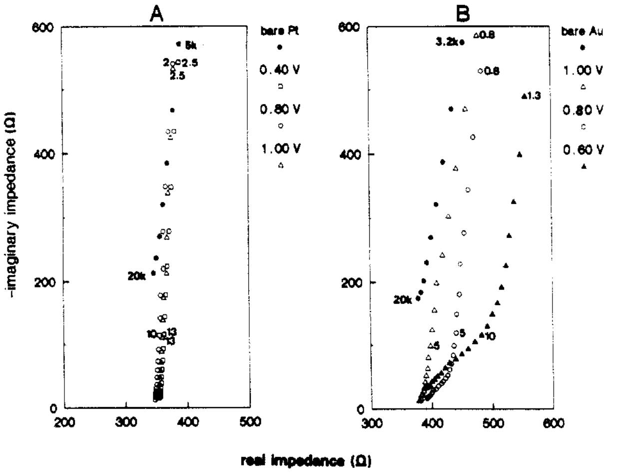

Figure 4. Complex plane impedance plots for poly-**Ib** (A, prepared in dichloromethane/Bu_4NClO_4; B, prepared in chloroform/Bu_4NPF_6) coated electrodes in acetonitrile containing Et_4NClO_4. Details and voltammograms are given in Figure 2 (B and C). Potentials and selected frequencies (Hz) are indicated. Measurements on bare electrodes were made at the open circuit potential.

Table I. Capacitances from Cyclic Voltammetry (CV) and Impedance Spectroscopy (IS) on a Poly-Ib (2 μM) Coated Pt Electrode in Acetonitrile Containing 0.2 M Et_4NClO_4

potential (V *vs* Ag/AgCl)	capacitance (mF)	
	IS	CV[a]
0.40	0.13	0.16
0.80	0.16	0.19
1.00	0.12	0.13

[a] Capacitance = average of anodic and cathodic current/scan rate.

acetonitrile. Cyclic voltammograms for this electrode, recorded prior to (···) and after (- - -) these impedance measurements, are shown in Figure 2C. The polymer is reasonably stable under the conditions of the impedance and voltammetric measurements. This film was prepared in the presence of Bu_4NClO_4 and appeared shiny. It is therefore assumed to have a compact, homogeneous morphology similar to that shown in Figure 3B.

In Figure 4A, the impedance plots for the poly-**Ib**-coated electrode all appear to be very similar to that of the bare electrode, except that the frequency range is much lower for the coated electrodes, indicating that they have a much higher capacitance. In all cases the almost vertical impedance plot indicates that the electrode behaves as a simple capacitor in series with a resistance. For the bare electrode this is its double-layer capacitance in series with the uncompensated solution resistance. The solution resistance can be estimated to be in the range 300–350 Ω by extrapolation to the real impedance (resistance) axis. The double-layer capacitance ($C = 1/\omega Z'' = 6.8 \times 10^{-8}$ F) was obtained from a plot of the imaginary impedance (Z'') *vs* 1/frequency (ω), which was linear. For the poly-**Ib**-coated electrode, the resistance (extrapolated to the real impedance axis) is almost the same as at the bare electrode, indicating that the polymer's resistance (ionic and electronic) is small. Capacitances from linear Z'' *vs* $1/\omega$ plots (Table I) are more than 3 orders of magnitude larger than that of the bare electrode, due to the Faradaic capacitance of the polymer, and are of a magnitude similar to capacitances estimated from a cyclic voltammogram recorded after the impedance measurements (Table I). For conducting polymers, it is normal for capacitances from cyclic voltammetry to be somewhat higher than those from impedance spectroscopy, although the reasons for this are not well understood.[40]

Table II. Resistances and Capacitances from the Impedance (IS) and Voltammetric (CV) Data Shown in Figures 2B and 4B for a Poly-Ib (3 μm) Coated Au Electrode

potential (V *vs* Ag/AgCl)	resistance (kΩ)	capacitance (mF)	
		IS	CV
1.00	0.09	0.36	
0.90	0.18	0.34	0.52
0.80	0.21	0.37	0.57
0.70	0.29	0.35	0.55
0.60	0.43	0.30	0.46
0.50	1.3	0.26	0.41
0.40	~6	0.24	0.29

The resistance of the 2-μm poly-**Ib** film is too low to measure from the impedance data shown in Figure 4, since it is clearly smaller than the uncertainty in the solution resistance. At the three potentials studied, the horizontal (real axis) offset from the bare electrode data is possibly as high as 30 Ω, which corresponds to a film resistance (electronic + ionic) of 90 Ω.[41] We can conclude that both the electronic and ionic conductivities of poly-**Ib** under these conditions are at least 3×10^{-4} S cm^{-1}.

Figure 4B shows complex plane impedance plots for a poly-**Ib** film prepared in chloroform. This film was prepared in the presence of Bu_4NPF_6 and was matt in appearance. It is therefore assumed to have a two-layer morphology similar to that shown in Figure 3A. Cyclic voltammograms for this electrode, recorded prior to the impedance measurements, are shown in Figure 2B.

In contrast to the film of similar thickness prepared in dichloromethane/Bu_4NClO_4 (Figure 4A), the film prepared in chloroform/Bu_4NPF_6 causes a shift of the low-frequency part of the impedance plot along the real impedance axis, relative to the data for the bare electrode. This means that the film exhibits a significant resistance, relative to the solution resistance, even at potentials as high as 1.0 V. At 0.8 and 0.6 V the data for the coated electrode fit a transmission line model that has been found to adequately represent the transient behavior of conducting polymers[37,42,43] and produces a complex impedance plot with a 45° linear region at high frequency and a 90° linear region at low frequency.[41] The high-frequency intercept with the real axis gives the uncompensated solution resistance plus a parallel combination of the polymer film's ionic and electronic resistances. The intercepts in Figure 4B are all close to the intercept for the bare electrode, indicating that either the polymer's ionic or electronic resistance is too small to accurately measure. The offset of the 90° low-frequency part of the impedance plot along the real impedance axis, relative to the data for the bare electrode, is then equal to a third of the film's total resistance (electronic and ionic). Plots of Z'' *vs* $1/\omega$ for data in this region provide the film's capacitance as described for the data in Figure 4A. Table II shows film resistances and capacitances from the impedance data shown in Figure 4B and some additional data at other potentials. Capacitances from cyclic voltammetry are also shown in Table II, and agreement with the values from the impedance measurements is again reasonable. The resistance of the film increases as the polymer is reduced (i.e., with decreasing potential), but the high-frequency intercept of the impedance plot remains close to the bare electrode value, indicating that either the ionic or electronic resistance of the polymer remains immeasurably low. Since it would be unreasonable to suggest that the reduced polymer retains significant electronic conductivity, we conclude that the polymer's ionic resistance is negligible at all potentials. The resistances given in Table II are

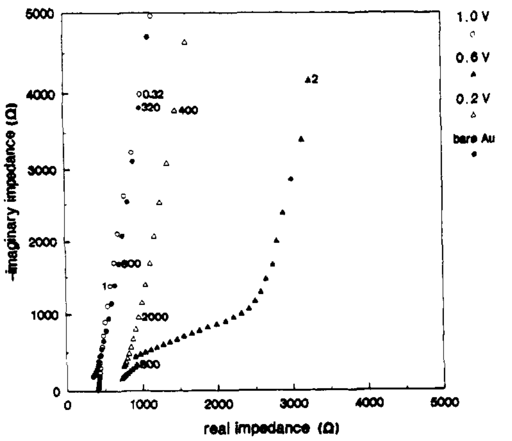

Figure 5. Complex plane impedance plots for a poly-**Ia**-coated Au electrode in acetonitrile containing Et_4NClO_4. Details and voltammograms are given in Figure 2A.

therefore electronic resistances, and the maximum electronic conductivity of this film is *ca.* 4 × 10^{-4} S cm^{-1} (at 1.0 V). Since this film presumably has a two-layer structure, this estimate of its conductivity represents an average for the two layers. At 0.4 V the conductivity is almost 2 orders of magnitude lower than the value observed at 1.0 V. At even lower potentials the impedance behavior becomes more complex and its treatment is beyond the scope of this paper.

Comparing the results in parts A and B of Figure 4, it appears that poly-**Ib** prepared in chloroform/Bu_4NPF_6 is significantly less conductive than poly-**Ib** prepared in dichloromethane/Bu_4NClO_4, at least at potentials below 1.0 V. The difference is at least a factor of 40 at 0.4 V and may be much higher. One factor responsible for this difference is clearly the lower redox potential of the material prepared in dichloromethane (see Figure 2). Other important factors could be more regular linkages, an increased average conjugation length, and the more compact morphology produced in the presence of Bu_4NClO_4.

Figure 5 shows complex plane impedance plots for a poly-**Ia**-coated Au electrode. This film was grown under the same conditions as that shown in Figure 3A and so presumably has a similar two-layer morphology. However, since it is significantly thinner (polymerization charge = 0.15 C cm^{-2}), there should be considerably less of the powdery outer layer.

As for the first poly-**Ib** film discussed above, this poly-**Ia** film behaves like a simple capacitor at 1.0 V and its resistance cannot be estimated. Its capacitance is similar to the value estimated by cyclic voltammetry. Thus poly-**Ia** has a maximum electronic conductivity of at least 10^{-4} cm^{-1}.

The impedance plot for the coated electrode at 0.2 V in Figure 5 is almost the same as that of the bare electrode except for an approximately 370-Ω offset along the real axis. The polymer film is completely reduced and does not increase the capacitance of the electrode significantly above the Pt double-layer value (note the similarity in frequencies for the bare Au (●) and 0.2 V (Δ) data in Figure (5). It merely impedes the access of ions to the Pt double layer and therefore increases the apparent solution resistance. The 370-Ω offset is the ionic resistance of the reduced poly-**Ia** film.[37,39] The ionic resistance of the oxidized film at 1.0 V is clearly much smaller than this because its impedance plot is not offset along the real axis (Figure 5). This is reasonable since the reduced polymer is expected to be neutral, while the oxidized form is cationic and contains mobile counteranions. At 0.6 V the polymer's impedance behavior does not fit the transmission line model particularly well because the high-frequency region is rather flat (it should be at 45°). However, the film exhibits a significant capacitance (0.02 mF) at this potential and clearly has a measurable electronic resistance. The offset of the low-frequency data along the real axis gives a resistance of *ca.* 8 kΩ and an electronic conductivity of 1 × 10^{-6} S cm^{-1}. At the same potential, the poly-**Ib** film prepared in chloroform had a significantly higher electronic conductivity of 8 × 10^{-5} S cm^{-1}. The difference can be attributed mainly to the lower redox potential of poly-**Ib**. To take this 300-mV difference into account, we should compare the conductivity of poly-**Ia** at 0.6 V with that of poly-**Ib** at 0.3 V. Although we could not directly determine the latter, we can estimate that it will be close to 1 × 10^{-6} S cm^{-1} based on the 0.4 V value of 6 × 10^{-6} S cm^{-1}.

Table III. *In situ* Electronic Conductivities from Dual-Electrode Voltammetry on Poly-Ib Films in Acetonitrile Containing 0.1 M Et_4NClO_4[a]

potential (V *vs* Ag/AgCl)	electronic conductivity (mS cm^{-1})	
	film A	film B
1.00		6
0.90		7
0.80	4	5
0.70	4	4
0.60	2	2
0.50	0.7	1
0.40	0.07	

[a] Film A (1 μm) was deposited from chloroform/Bu_4NClO_4 onto a Pt disk. It was coated with a gold film to provide the second electrical contact. Film B (4 μm) was deposited from dichloromethane/Bu_4NClO_4 onto two parallel band electrodes.

Dual-Electrode Voltammetry. Since the maximum electronic conductivities of poly-**Ia** and poly-**Ib** are too high to be accurately determined by impedance spectroscopy, two types of dual-electrode voltammetry were also used. In one type of experiment, a porous gold film serves as an electronic contact to the surface of the polymer film on a Pt disk electrode.[27,44] In the other, the polymer film is grown on two adjacent parallel band electrodes until it bridges the gap between them.[28] In situ electronic conductivity measurements are made by applying a small (20 mV) potential difference across the film while it is immersed in an electrolyte solution. The electronic resistance of the film is calculated from the steady-state current using Ohm's law. Conductivity measurements can be made at any selected potential relative to the reference electrode.

Results for two experiments on poly-**Ib** are presented in Table III. Although the two films were grown from different solvents, their conductivities agree remarkably well. The maximum conductivity of poly-**Ib** is ca. 7 × 10^{-3} S cm^{-1}.

The results given in Table III clearly show that the large differences observed in the impedance results for poly-**Ib** (Figure 4) are due primarily to the electrolyte. It appears that the high electronic resistances observed in the impedance spectroscopy of poly-**Ib** prepared in chloroform/Bu_4NPF_6 (Table II) include a large contribution from the powdery outer layer.

Conclusions

Bithiazole-containing polymers prepared by electrochemical polymerization of **Ia** and **Ib** exhibit good conductivities and stable electrochemistry in acetonitrile. The maximum conductivity of poly-**Ib** is close to 0.01 S cm^{-1}.

On the basis of results in the literature for thienylene–phenylene copolymers,[45] the electronic properties of poly-**Ia** should be intermediate between those of polythiophene and poly(4,4′-dimethyl-2,2′-bithiazole). The ionization potential of poly[5,5′-(2,2′-bithiazole)] has been estimated to be *ca.* 0.22 eV higher than that of polythiophene.[6] The anodic peak potential of 0.72 V *vs* SSCE for poly(bithiophene) probably gives the best estimate of the redox potential of the ideal polythiophene structure because polythiophene itself (anodic peak potential ~0.96 V) gives a very asymmetric voltammogram.[46] On the basis of these data, poly-**Ia** would be predicted to exhibit an anodic peak at *ca.* 0.77 V *vs* our Ag/AgCl electrode. The voltammogram shown in Figure 2A matches this prediction reasonably well, suggesting that we have produced a regular 2,5-linked bithiazole/bithiophene copolymer. The nitrogen atoms introduced into the conduction pathway appear to have decreased the conductivity significantly relative to polythiophene (*ca.* 100 S cm^{-1}).[32] However, the maximum conductivity of poly-**Ib** is comparable to that of poly(α-terthiophene),[32] indicating that other factors are probably responsible for its low conductivity relative to polythiophene.

The methoxy substituents on **Ib** produce several advantages over **Ia**. First, they increase its solubility, thereby allowing a choice of solvents for the polymerization and more opportunity for optimization of the polymer's properties. Second, the electron-donating effect of the methoxy groups lowers the polymerization potential and therefore reduces the risk/extent of oxidative degradation during the polymerization. The methoxy substituents also lower the redox potential of the resulting polymer, so that it becomes conductive at lower potentials.

Acknowledgment. Financial support from the Natural Sciences and Engineering Research Council of Canada (NSERC) and Memorial University is gratefully acknowledged.

References and Notes

(1) Krivoshei, I. V.; Skorobogatov, V. M. *Polyacetylene and Polyarylenes. Synthesis and Conductive Properties*; Polymer Monographs Vol. 10; Gordon and Breach: Philadelphia, 1991.

(2) Heinze, J. In *Topics in Current Chemistry*; Springer-Verlag: Berlin, 1990; Vol. 152, pp 1–47.

(3) Kaneko, M.; Wohrle, D. *Adv. Polym. Sci.* **1988**, *84*, 141–228.

(4) Techagumpuch, A.; Nalwa, H. S.; Miyata, S. In *Electroresponsive Molecular and Polymeric Systems*; Skotheim, T. A., Ed.; Marcel Dekker: New York, 1991; Vol. 2, pp 257–294.

(5) Naarmann, H.; Theophilou, N. In *Electroresponsive Molecular and Polymeric Systems*; Skotheim, T. A., Ed.; Marcel Dekker: New York, 1988; Vol. 1, pp 1–39.

(6) Catellani, M.; Destri, S.; Porzio, W.; Themans, B.; Bredas, J. L. *Synth. Met.* **1988**, *26*, 259–265.

(7) Bolognesi, A.; Catellani, M.; Destri, S.; Porzio, W. *Synth. Met.* **1987**, *18*, 129–132.

(8) Aldissi, M.; Nyitray, A. M. *ACS Symp. Ser.* **1987**, *346*, 559–567.

(9) Bredas, J.-L. In *Handbook of conducting polymers*; Skotheim, T. A. Ed.; Marcek Dekker: New York, 1986; Vol. 2, pp 859–913.

(10) Tanaka, S.; Kaeriyama, K. *Makromol. Chem., Rapid Commun.* **1988**, *9*, 743–748.

(11) Deronzier, A.; Moutet, J.-C. *Acc. Chem. Res.* **1989**, *22*, 249–255.

(12) Funaki, H.; Aramaki, K.; Nishihara, H. *Chem. Lett.* **1992**, 2065–2068.

(13) Czerwinski, A.; Cunningham, D. D.; Amer, A.; Schrader, J. R.; Pham. C. V.; Zimmer, H.; Mark, H. B., Jr.; Pons, S. *J. Electrochem. Soc.* **1987**, *134*, 1158–1164.

(14) Gourier, D.; Tourillon, G. *J. Phys. Chem.* **1986**, *90*, 5561–5565.

(15) Tanaka, S.; Sato, M.-A.; Kaeriyama, K. *J. Macromol. Sci., Chem.* **1987**, *A24*, 749–761.

(16) Pelter, A.; Maud, J. M.; Jenkins, I. H.; Sadeka, C.; Coles, G. *Tetrahedron Lett.* **1989**, *30*, 3461.

(17) Reynolds, J. R.; Ruiz, J. P.; Child, A. D.; Nayak, K.; Marynick, D. S. *Macromolecules* **1991**, *24*, 678–687.

(18) Ruiz, J. P.; Dharia, J. R.; Reynolds, J. R.; Buckley, L. J. *Macromolecules* **1992**, *25*, 849–860.

(19) Chang, A.-C.; Blankespoor, R. L.; Miller, L. L. *J. Electroanal. Chem.* **1987**, *236*, 239–252.

(20) Jen, K.-Y.; Eckhardt, H.; Jow, T. R.; Shacklette, C. W.; Elsenbaumer, R. L. *J. Chem. Soc., Chem. Commun.* **1988**, 215.

(21) Waltman, R. J.; Bargon, J. *Can. J. Chem.* **1986**, *64*, 76–95.

(22) Negishi, E.; King, A. O.; Okuda, N. *J. Org. Chem.* **1977**, *42*, 1821.

(23) Minato, A.; Tamao, K.; Hayashi, T.; Suzuki, K.; Kumada, M. *Tetrahedron Lett.* **1980**, *21*, 845.

(24) Pelter, A.; Rowlands, M.; Jenkins, I. H. *Tetrahedron Lett.* **1987**, *28*, 5213.

(25) Karrer, P.; Lieser, P.; Graf, W. *Helvetica* **1944**, *27*, 489.

(26) Audisio, G.; Catellani, M.; Destri, S.; Pelli, B.; Troldi, P. *J. Heterocycl. Chem.* **1990**, *27*, 463.

(27) Mao, H.; Pickup, P. G. *Chem. Mater.* **1992**, *4*, 642–645.

(28) Schiavon, G.; Sitran, S.; Zotti, G. *Synth. Met.* **1989**, *32*, 209.

(29) Bartlett, P. N.; Chung, L.-Y.; Moore, P. *Electrochimica Acta* **1990**, *35*, 1273–1278.

(30) Pickup, P. G.; Osteryoung, R. A. *J. Am. Chem. Soc.* **1984**, *106*, 2294–2299.

(31) Heinze, J.; Storzbach, M.; Mortensen, J. *Ber. Bunsenges. Phys. Chem.* **1987**, *91*, 960–967.

(32) Roncali, J. *Chem. Rev.* **1992**, *92*, 711–738.

(33) Reynolds, J. R.; Hsu, S.-G.; Arnott, H. J. *Polym. Sci., Part B: Polym. Phys.* **1989**, *27*, 2081–2103.

(34) Lang, P.; Chao, F.; Costa, M.; Lheritier, E.; Garnier, F. *Ber. Bunsen-Ges. Phys. Chem.* **1988**, *92*, 1528–1536.

(35) Tourillon, G. In *Handbook of Conducting Polymers*; Skotheim, T. A., Ed.; Marcel Dekker: New York, 1986; Vol. 1, pp 293–350.

(36) Qi, Z.; Pickup, P. G. *Anal. Chem.* **1993**, *65*, 696–703.

(37) Ren, X.; Pickup, P. G. *J. Chem. Soc., Faraday Trans.* **1993**, *89*, 321–326.

(38) Duffitt, G. L.; Pickup, P. G. *J. Chem. Soc., Faraday Trans.* **1992**, *88*, 1417–1423.

(39) Pickup, P. G. *J. Chem. Soc., Faraday Trans.* **1990**, *86*, 3631–3636.

(40) Tanguy, J.; Baudoin, J. L.; Chao, F., Costa, M. *Electrochim. Acta* **1992**, *37*, 1417–1428.

(41) Albery, W. J.; Elliott, C. M.; Mount, A. R. *J. Electroanal. Chem.* **1990**, *288*, 15–34.

(42) Albery, W. J.; Chen, Z.; Horrocks, B. R.; Mount, A. R.; Wilson, P. J.; Bloor, D.; Monkman, A. T.; Elliott, C. M. *Faraday Discuss. Chem. Soc.* **1989**, *88*, 247–259.

(43) Mao, H.; Ochmanska, J.; Paulse, C. D.; Pickup, P. G. *Faraday Discuss. Chem. Soc.* **1989**, *88*, 165–176.

(44) Pickup, P. G.; Kutner, W.; Leidner, C. R.; Murray, R. W. *J. Am. Chem. Soc.* **1984**, *106*, 1991–1998.

(45) Montheard, J. P.; Pascal, T.; Seytre, G.; Steffan-Boiteux, G.; Douillard, A. *Synth. Met.* **1984**, *9*, 389.

(46) Waltman, R. J.; Bargon, J.; Diaz, A. F. *J. Phys. Chem.* **1983**, *87*, 1459–1463.